

# Effects of longitudinal parasitic modes on the beam dynamics for the ADS driving linac in China

CHENG Peng(程鹏)<sup>1</sup> PEI Shi-Lun(裴士伦) WANG Jiu-Qing(王九庆)

LI Zhi-Hui(李智慧) TANG Jing-Yu(唐靖宇)

Institute of High Energy Physics, Chinese Academy of Sciences, Beijing 100049, China

**Abstract:** For the accelerator driven subcritical system (ADS) main linac in China, two families of superconducting elliptical radio frequency (RF) cavities will be used to accelerate the proton beam from 180 MeV to 1.5 GeV. When the proton beam traverses in the RF cavity, the excited parasitic modes, like high order modes (HOMs) and same order modes (SOMs), may drive the beam to become unstable and increase the cryogenic load, thus putting a limitation on the normal operation of the accelerator. In this paper, by using a numerical code SMD based on the ROOT environment, the effects of longitudinal parasitic modes on the beam dynamics for the ADS driving linac in China have been investigated systematically, while parasitic modes which increase cryogenic loss have not been included in this paper. Some conclusions concerning the beam energy ranging from 180 MeV to 1.5 GeV have been obtained.

**Key words:** parasitic mode, HOM, SOM, beam dynamics, beam instability

**PACS:** 29.27.Bd **DOI:** 10.1088/1674-1137/39/1/017005

## 1 Introduction

The accelerator driven subcritical system (ADS) project in China [1] aims to build an accelerator driven sub-critical system around the year of 2032. By using superconducting accelerating structures, except for the RFQs, the driving accelerator runs in continuous wave (CW) mode and accelerates the 10 mA proton beam from 35 keV at the electron cyclotron resonance (ECR) ion source exit to 1.5 GeV to bombard the target to produce neutrons. Fig. 1 shows the general layout of the ADS driver linac. To satisfy the restrictive requirement on stability and reliability in the low energy part, there are two identical injectors operating in parallel, acting as a hot spare for each other.

Based on the 10 MeV/325 MHz Injector I testing facility constructed at IHEP, the main specifications of the ADS driver linac can be summarized in Table 1. It can be seen that the ADS driver linac has very high beam power and very high reliability, which are not possessed by any of the existing proton linacs in the world.

When the particle beam traverses in the radio frequency (RF) cavity, the excited high order modes (HOMs) and same order modes (SOMs) may drive the beam to become unstable, thus putting a limitation on the normal operation of the accelerator [2, 3]. Especially for high power superconducting linacs, beam induced parasitic modes may also increase the cryogenic load. In very serious cases a quench may happen and

the machine's operation might be interrupted. Thus, it is necessary to evaluate the effects of beam excited HOMs and SOMs in the ADS driver linac.

This paper is only concerned with the effects of longitudinal parasitic modes on the beam dynamics within superconducting section from 180 MeV to 1.5 GeV. For this energy range there are two families of superconducting elliptical cavities, the parameters are listed in Table 2.

Table 1. Main specifications of the ADS driver linac.

parameter	value
operating mode	CW
final kinetic energy/GeV	1.5
beam current/mA	10
beam duty factor(%)	100
bunch frequency/MHz	325
beam power at target/MW	15
RF frequency/MHz	325/650
beam loss/(W/m)	<1
	<25000(1 s<t<10 s)
beam trips per year	<2500(10 s<t<5 min)
	<25(5 min<t)

Table 2. Parameters of superconducting elliptical cavities.

parameter	medium $\beta$	high $\beta$
# of cells	5	5
frequency/MHz	650	650
geometric $\beta_g$	0.63	0.82
$R/Q@\beta_g/\Omega$	321.7	512.4

Received 17 February 2014

1) E-mail: chengp@ihep.ac.cn

©2015 Chinese Physical Society and the Institute of High Energy Physics of the Chinese Academy of Sciences and the Institute of Modern Physics of the Chinese Academy of Sciences and IOP Publishing Ltd

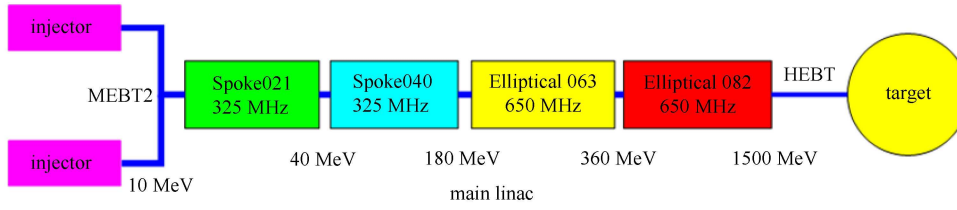


Fig. 1. The general layout of the ADS driver linac.

## 2 Basic theory

When a point charge travels through an RF cavity along the beam axis, monopole modes will be excited. According to the fundamental theorem of beam loading [4], the net induced voltage for one monopole mode by a point charge  $q$  can be given by

$$\Delta V_{q,n} = -q \frac{\omega_m}{2} \left( \frac{R}{Q} \right)_n (\beta), \quad (1)$$

where  $\omega_n$  is the angular frequency of the mode and  $\beta$  is the normalized particle velocity.  $(R/Q)_n$  is defined as

$$\left( \frac{R}{Q} \right)_n (\beta) = \frac{\left| \int_{-\infty}^{\infty} E_{z,n}(r=0, z) e^{i\omega_n(z/\beta c)} dz \right|^2}{\omega_n U_n}, \quad (2)$$

where  $U_n$  is the stored energy of the specific mode  $n$ ,  $E_z(r=0, z)$  is the RF electric field component along the beam axis. As time evolves, the voltage of mode  $n$  will decay exponentially due to wall power loss,

$$V_n(t) = \Delta V_{q,n} e^{-t/T_{d,n}} e^{i\omega_n t}, \quad (3)$$

where  $T_{d,n} = 2Q_{L,n}/\omega_n$  is the decay time constant. Here,  $Q_L$  is the loaded quality factor with definition of

$$\frac{1}{Q_{L,n}} = \frac{1}{Q_{0,n}} + \frac{1}{Q_{\text{ex},n}}. \quad (4)$$

$Q_{0,n}$  and  $Q_{\text{ext},n}$  are the unloaded and external quality factor of mode  $n$ , respectively. For the superconducting RF cavity,  $Q_{0,n}$  is at the order of  $10^{10}$ , which is much higher than  $Q_{\text{ext},n}$ ; therefore,  $Q_{L,n}$  can be approximated by  $Q_{\text{ext},n}$ .

At the same time as mode excitation, the point charge  $q$  will also experience an energy change,

$$\Delta U_n = q \cdot \left[ R(V_n) \cos(\omega_n dt) - I(V_n) \sin(\omega_n dt) - \frac{1}{2} \Delta V_{q,n} \right], \quad (5)$$

where  $R(V_n)$  and  $I(V_n)$  stand for the real and imaginary part of the monopoles' voltage excited by the earlier passed point charges. In the meantime, half of the self-excited voltage  $\Delta V_{q,n}$  by the point charge will also act back on itself.

Taking into account the RF power sources errors, the energy gain difference between the point particle and the

synchronous particle can be represented as

$$\Delta U_{\text{RF}} = q V_{\text{RF}}^* \cos(\varphi_s^* + \omega_{\text{RF}} dt) - q V_0 \cos(\varphi_s), \quad (6)$$

where  $V_{\text{RF}}^*$  is the RF cavity voltage including the RF amplitude error,  $\varphi_s^*$  is the RF phase including error, and  $dt$  is the particle's arrival time error.

For one charged particle, the total energy error through a cavity  $m$  can be given by

$$\Delta E^{(m+1)} = \Delta E^{(m)} + \Delta U_{\text{RF}}^{(m)} + \Delta U_n^{(m)}, \quad (7)$$

where  $\Delta U_n^{(m)}$  and  $\Delta U_{\text{RF}}^{(m)}$  are the energy errors developed by the beam induced monopole mode and the RF in RF cavity  $m$ , respectively.  $\Delta E^{(m)}$  is the energy error already present before the point charge enters into the RF cavity  $m$ .

As is well known, when the charged particle passes through the drift between two neighbouring RF cavities, the energy error will result in an arrival time error, which can be written as

$$\Delta t^{(m+1)} = \Delta t^{(m)} + (dt/dE)_E^{(m)} \cdot \Delta E^{(m)}, \quad (8)$$

where

$$(dt/dE)_E^{(m)} = -\frac{L(m)}{c^3 \cdot (\gamma^2 - 1)^{3/2} m_0} \cdot L^{(m)}$$

is the drift length between RF cavities  $m$  and  $m+1$ ,  $c$  is the speed of light,  $\gamma$  and  $m_0$  are the particle's relativistic factor and rest mass.

## 3 Simulation execution

### 3.1 Methodology

In this paper, numerical code SMD [5] is used to study the monopole modes' effects on the beam dynamics. The code has two logical modules: one for the longitudinal plane and another for the transverse plane. Because the SMD code is based on the ROOT [6] environment, it allows for a very fast simulation speed, and the powerful data analysis routines in the framework can be used to deal with the mass output data. For the CW beam, many more bunches than the pulsed beam are needed in one run, so the beam excited field can reach a steady state in the RF cavity.

In SMD, the drift-kick-drift model [8] is used to model the beam and cavity interaction. At the mid-plane of

each cavity, the particle will interact with the cavity. Thus, the linac can be modeled as a series of drifts and kicks. Point like bunches are tracked through each linac, which means that only a multi-bunch instead of a single bunch effect is studied. It is worth pointing out that the space charge effects are not considered in any of the simulations conducted by SMD.

### 3.2 Monopole mode analysis

For the energy range from 180 MeV to 1.5 GeV that is studied in this paper, two types of superconducting elliptical 5-cell cavities with  $\beta=0.63$  and  $\beta=0.82$  are adopted. With CST MWS [7], the characteristics of the monopole SOMs and HOMs are analyzed, the results of which will be used to evaluate their effects on the beam dynamics. Fig. 2 shows the  $R/Q$  of the HOMs and SOMs as a function of the particle velocity for the  $\beta=0.63$  cavity, while Fig. 3 shows the  $\beta=0.82$  cavity. All of the modes listed here are below the beam pipe cut-off frequency. Trapped modes with much higher frequency are not considered in this paper, while there may exist dangerous ones.

Because of the  $R/Q$  dependence on the varying particle velocity, it is very hard to include all of the modes in

the simulation, and the HOM and SOM with the highest overall  $R/Q$  in each section are chosen as the default for all simulations. For example, the 1646 MHz and 1345 MHz HOM modes in the  $\beta=0.63$  and  $\beta=0.82$  sections are selected. According to the experience at DESY and Jefferson Laboratory [8], the RMS width of the Gaussian distributed HOM frequency spread is commonly a 1 MHz spread, but a default value of 100 kHz is used as a conservative assumption in this paper.

It is worth pointing out that one should keep in mind that the  $R/Q$  will change significantly if the mechanical imperfection is concerned [9]; therefore, our simulations are carried out with a conservative assumption and safety margin to include this effect.

### 3.3 Simulation results

The effects of longitudinal parasitic modes on the beam dynamics in the ADS driver linac are studied in three cases.

1) The HOM parameters obtained in Section 3.2 are used (i.e., the 1646 MHz and 1345 MHz modes with the highest overall  $R/Q$ ).

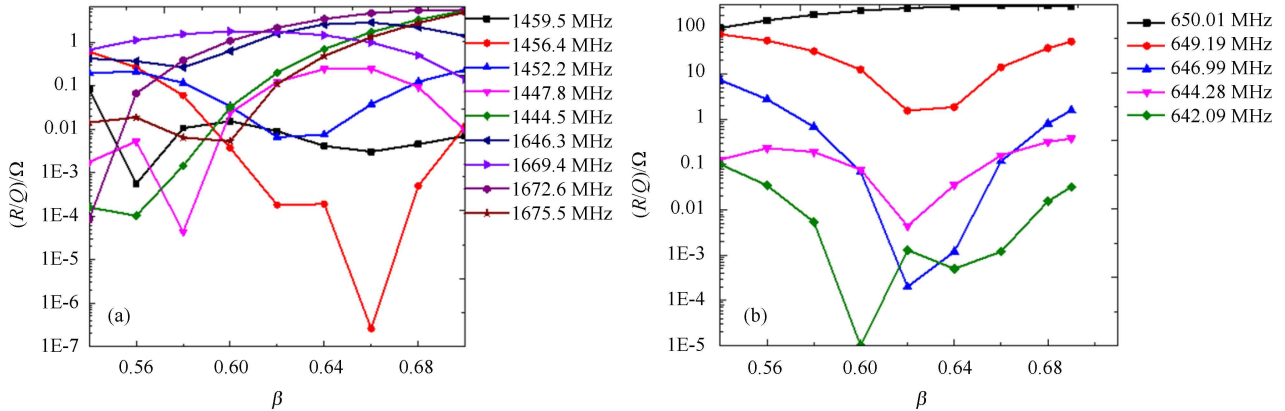


Fig. 2. The  $R/Q$  of the HOMs (a) and SOMs (b) as a function of the particle velocity for the  $\beta=0.63$  cavity.

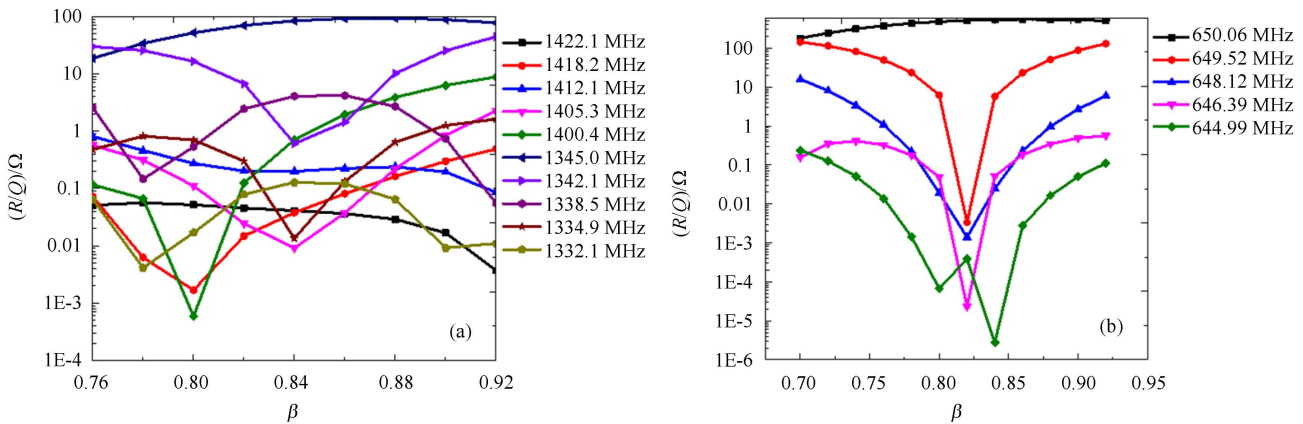


Fig. 3. The  $R/Q$  of the HOMs (a) and SOMs (b) as a function of the particle velocity for the  $\beta=0.82$  cavity.

2) The HOMs are sitting on the machine line, the frequency of which is a multiple of the bunch frequency.

3) The SOM parameters presented in Section 3.2 are considered.

For the SMD simulation on the CW proton beam existing in the ADS driver linac, 650 k bunches are launched to the  $\beta=0.63$  section entrance. At the end of each run, both the energy and phase errors of all the 650 k bunches at the linac end are stored and analysed.

To facilitate the evaluation of the monopole parasitic modes' effects, the phase space area created by all bunches can be defined as

$$\varepsilon = \pi \sqrt{\langle dE^2 \rangle \langle d\varphi^2 \rangle - \langle dE d\varphi \rangle^2} \quad (9)$$

where  $dE$  and  $d\varphi$  are the energy error and phase error, respectively.

To quantitatively study the effects of the HOMs and SOMs in the ADS driver linac, the nominal beam with injection energy and phase jitters listed in Table 3 is simulated first. The resulting multi-bunch phase space at the linac end is shown in Fig. 4.

Table 3. Beam input parameters with jitter effects.

parameter	value	$\sigma$
input energy/MeV	180	0.078
phase/(°)	-25--12	0.4
beam current/mA	10	3%

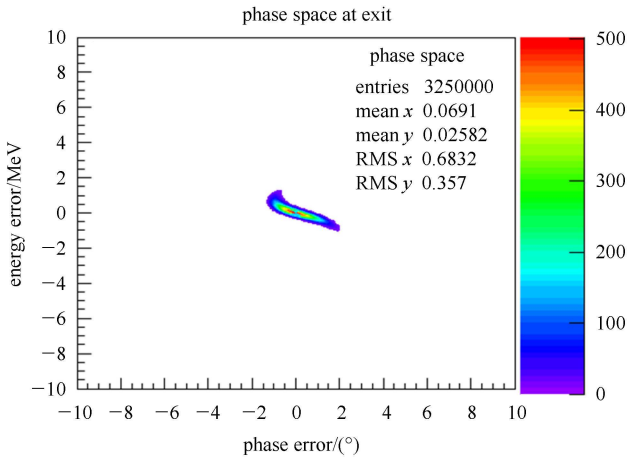


Fig. 4. Phase space at the linac end for the nominal beam with only injection energy and phase jitters.

The RF power sources errors will cause additional energy and phase jitter at the linac end. The design goal of the RMS RF power sources errors in the ADS driver linac is to reach  $\pm 0.5^\circ$  in phase and  $\pm 0.5\%$  in amplitude. With these errors, 100 different linacs are simulated to study the effect of RF power sources errors statistically. Fig. 5 shows the phase space at the exit of 100 linacs

with uniformly distributed RF power sources errors. It can clearly be seen that the phase space area  $\varepsilon$  grows compared with the case without RF power sources errors present. If the phase space shown in Fig. 5 is normalized to that in Fig. 4, then an average emittance growth factor of  $\varepsilon_{\text{RF}}/\varepsilon=2.8$  can be obtained, which can be defined as the tolerable limit of the longitudinal parasitic modes induced beam performance dilution. The RF power sources errors caused emittance growth rate is  $\varepsilon_{\text{RF}}/\varepsilon-1=1.8=180\%$ .

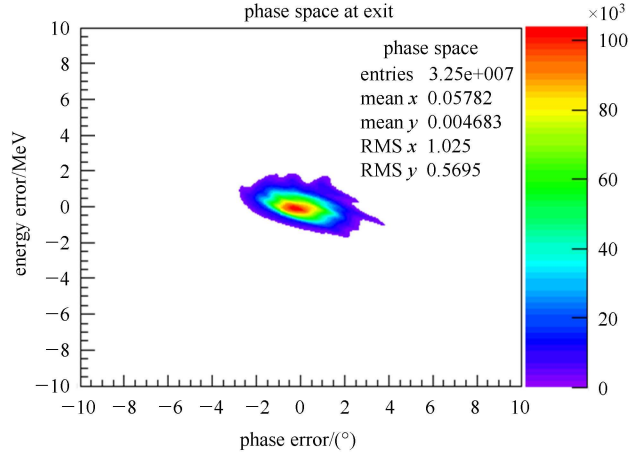


Fig. 5. Phase space at the exit of 1000 linacs with uniformly distributed RF power sources errors.

### 3.3.1 Effects of HOMs from CST MWS simulation

Here only the HOMs with the highest overall  $R/Q$  are considered. The 1646 MHz mode with average  $R/Q=10 \Omega$  at  $\beta=0.63$  section and the 1345 MHz one with average  $R/Q=70 \Omega$  at  $\beta=0.82$  section are used in the SMD simulation, both of them are far away from the machine line. By varying the beam current,  $Q_{\text{ext}}$  and the HOMs' frequency spread, 100 linacs are simulated with a different seed HOM frequency generator, while all of the other parameters remain constant.

The results of the average and maximum phase space growth of the 100 linacs with varying beam current and  $Q_{\text{ext}}$  are shown in Fig. 6. The adopted Gaussian HOM frequency spread is  $\sigma=100$  kHz. No bunches are lost in any of the simulations. Even for 10 times the nominal beam current, the phase space growth  $\varepsilon_{\text{HOM}}/\varepsilon$  is almost negligible, even when  $Q_{\text{ext}}$  reaches  $10^9$  based on the tolerable limit. Therefore, it can be concluded that the effects of the HOMs with the overall highest  $R/Q$  on the longitudinal beam dynamics are not severe for the ADS driver linac in the energy range of 180 MeV to 1.5 GeV.

It is found that the HOM frequency spread plays an important role in the HOM effects on the longitudinal beam dynamics [10], thus the dependence on the frequency spread is also investigated. Fig. 7 shows the simulation results. The RMS width of the Gaussian distrib-

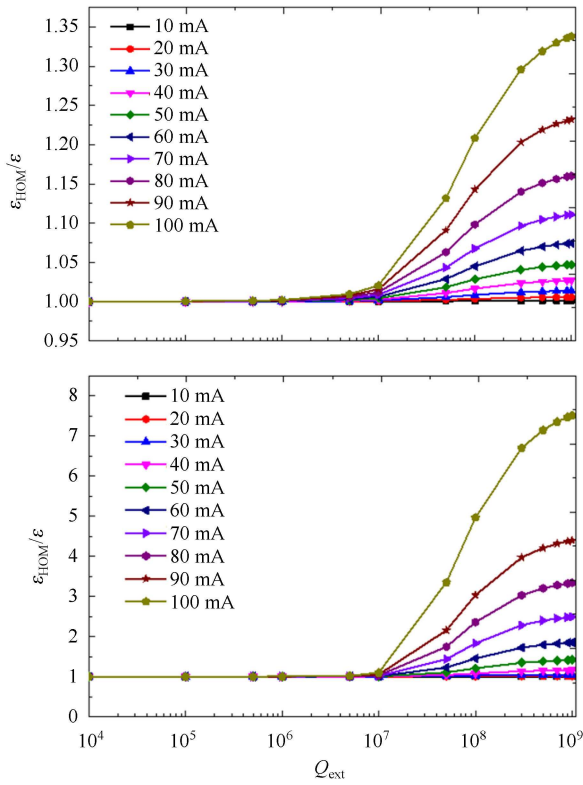


Fig. 6. The average and maximum phase space growth against the  $Q_{\text{ext}}$  and the beam current.

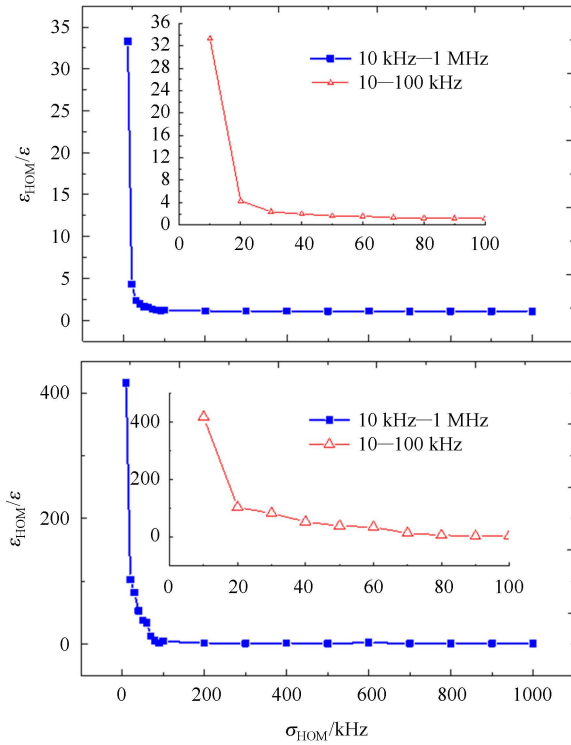


Fig. 7. The average and maximum phase space growth against the HOM frequency spread.

uted HOM frequency spread  $\sigma$  varies from 10 kHz to 1 MHz with 100 mA beam current (as the safety margin) and  $Q_{\text{ext}}=10^8$ . As one can see, the phase space growth due to HOMs is less obvious and can be ignored when  $\sigma$  is larger than 100 kHz. Based on the empirical results, the frequency spread of any mode can be estimated by  $\sigma = 1.09 \times 10^{-3} \cdot |f_n - f_0|$  [11], where  $f_n$  is the mode's frequency of interest and  $f_0$  is the frequency of the fundamental accelerating mode. Then, the derived HOM frequency spread width for the  $\beta=0.63$  and  $\beta=0.82$  sections in the ADS driver linac is much larger than 100 kHz.

### 3.3.2 Effects of HOMs sitting on the machine line

HOMs lying on a machine line are the most dangerous situation. For the  $\beta=0.63$  and  $\beta=0.82$  sections in the ADS driver linac, simulations for two scenarios are carried out.

1) The mean HOM frequency is set to be 1625 MHz, which is five times the bunch frequency. The RMS frequency spread width varies from 10 kHz to 1 MHz.

2) Based on 1), the HOM damping is also considered with the RF power sources errors present.

The same as before, 100 linacs are simulated for statistical reasons. Fig. 8 shows the case corresponding to scenario a) at a beam current 100 mA as safety margin and  $Q_{\text{ext}}=10^8$  (i.e., no HOM coupler present). The phase space growth increases as the RMS frequency spread changes from 10 kHz to 100 kHz, this is mostly because most bunches are lost in this range. For this reason, the beam current is re-set to the nominal 10 mA, the result of which is shown in Fig. 9. It can be seen that even when no HOM coupler is present, the HOMs sitting on the machine line can also be damped at the 10 mA nominal beam current. The precondition is that the RMS width of the Gaussian distributed frequency spread is larger than 1 MHz.

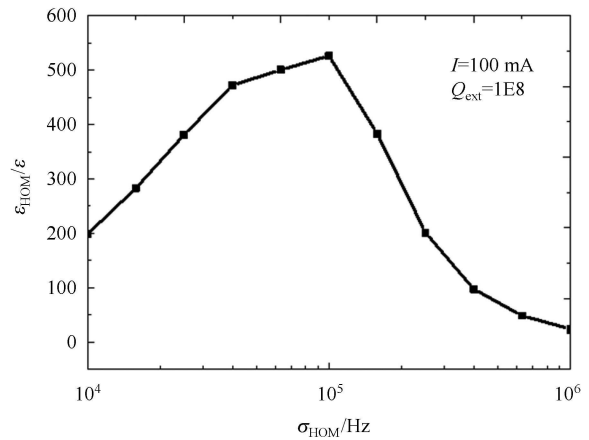


Fig. 8. The average phase space growth for 100 mA beam current and HOMs sitting on machine line with  $Q_{\text{ext}}=10^8$ .

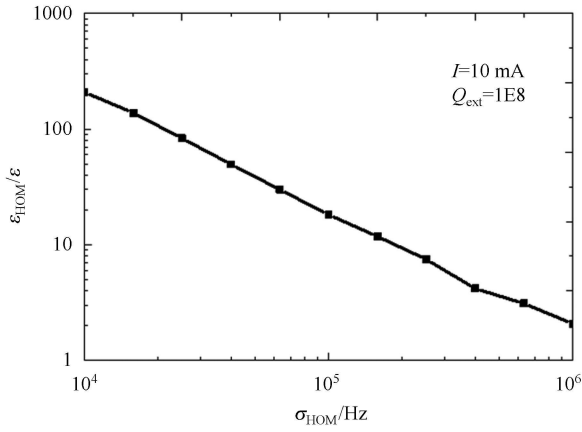


Fig. 9. The average phase space growth for 10 mA beam current and HOMs sitting on machine line with  $Q_{\text{ext}}=10^8$ .

Figure 10 shows the results corresponding to scenario 2). The compared situations include the HOMs sitting on the machine line (ML), the machine line plus the effect of the RF power sources errors (ML+RF) and only RF power sources errors (RF) present. The solid line depicts the maximum phase space growth, while the dotted one is for the average. The beam current and the HOM frequency spread width are set to be 10 mA and 1 MHz, respectively. The RF power sources errors have uniform distributions with  $\pm 0.5^\circ$  in phase and  $\pm 0.5\%$  in amplitude. One can see that, the average phase space growth caused by the ML is much less than that caused by ML+RF when  $Q_{\text{ext}}$  is less than  $10^6$ , hence the RF power source errors play a more important role in the phase space growth when the machine line induced effects are negligible.

### 3.3.3 Effects of SOMs

Compared with the HOMs, the SOMs have relatively

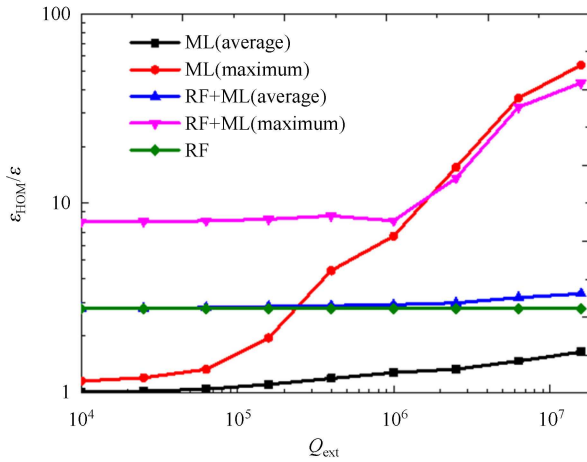


Fig. 10. The average and the maximum phase space growth including both the RF power sources errors and machine line.

larger overall  $R/Q$ , which is shown in Figs. 2 and 3. However, the mode frequency spread is lower.

Due to the largest  $R/Q$  among the TM<sub>010</sub> SOM pass band,  $4\pi/5$  mode is used in the studies on the ADS driver linac. The mode frequency spread is set to be around 1 kHz. The result obtained by varying the beam current and  $Q_{\text{ext}}$  is shown in Fig. 11. It can be seen that the phase space growth is not so obvious if the  $Q_{\text{ext}}$  is less than  $10^6$ , even for a beam current of 100 mA. Generally speaking, the fundamental RF mode coupler also provides a damping for the SOMs [12], while the damping  $Q_{\text{ext}}$  is usually at the order of  $10^5$ – $10^6$ , which is sufficient to suppress the effects induced by the SOMs.

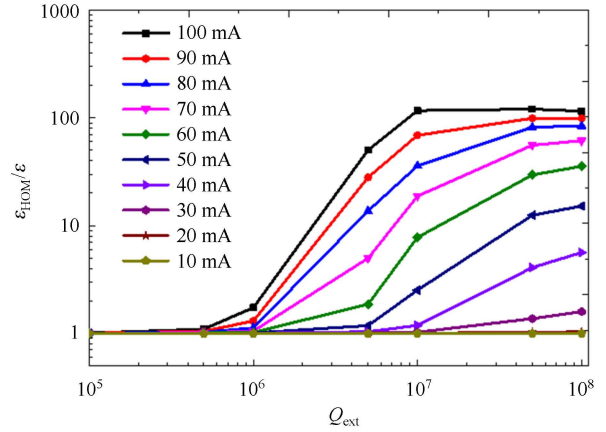


Fig. 11. The average phase space growth against  $Q_{\text{ext}}$  and the beam current.

## 4 Conclusions

In this paper, the effects of longitudinal parasitic modes on the beam dynamics in the  $\beta=0.63$  and  $\beta=0.82$  sections (180 MeV to 1.5 GeV) of the ADS driver linac have been studied systematically.

These modes should not be a problem when the HOMs' frequencies are far away from the machine line, even when the  $Q_{\text{ext}}$  is at  $10^9$  and when the beam current is increased to 100 mA. For the 10 mA nominal beam current, those modes sitting on the machine line are of little concern, but only if the RMS HOM frequency spread is larger than 1 MHz. It is found that the frequency spread offers an additional detuning effect, which is beneficial to the longitudinal beam dynamics. Normally, the RMS width of the Gaussian distributed frequency spread is around 1 MHz for the HOMs, which is sufficient. Therefore, HOMs couplers may not be required for the nominal operation of the  $\beta=0.63$  and  $\beta=0.82$  sections in the ADS driver linac.

For the SOMs, because the  $Q_{\text{ext}}$  provided by the fundamental RF power coupler is at the order of  $10^5$ – $10^6$ , the SOMs effects can be successfully suppressed.

Based on the simulations conducted in this paper, the longitudinal beam instability induced by the HOMs and SOMs has little effect on the longitudinal beam performance for the current ADS main linac design because the modes existing in the  $\beta=0.63$  and  $\beta=0.82$  elliptical cavities are far away from the machine line and their  $R/Q$  values are much smaller compared with the funda-

mental accelerating mode. In the meantime, the RMS frequency spreads of the HOMs and SOMs are also large enough to further suppress the longitudinal instability.

*The authors would like to thank all the colleagues in the ADS beam dynamics group for helpful discussions and Marcel Schuh for his generous offer of the SMD code.*

## References

- 1 TANG J Y, LI Z H et al. Conceptual Physics Design on the C-ADS Accelerators. IHEP-CADS-Report/2011-1E
- 2 Gluckstern R L, Cooper R K. Proceedings of PAC 1985. IEEE Trans. Nucl. Sci., 1985, 32
- 3 Jeon D, Merminga L et al. Nucl. Instrum. Methods Phys. Res., Sect. A, 2002, **495**: 85
- 4 Wilson P B, Griffin J E. AIP Conference Proceedings, 1982, **87**(1): 450. <http://dx.doi.org/10.1063/1.33620>
- 5 Simulate Higher Order Mode Dynamics (SMD) Code Repository. <https://svnweb.cern.ch/trac/splhombbu>
- 6 Brun R, Rademakers F. ROOT-An Object Oriented Data Analysis Framework. Proceedings AIHENP'96 Workshop. Lausanne, Sep. 1996. (Nucl. Instrum. Methods in Phys. Res. A, 1997, **389**: 81–86. <http://root.cern.ch/>)
- 7 Computer Simulation Technology (CST). Homepage (2010. 10. 06). [www.cst.com](http://www.cst.com)
- 8 Marcel Schuh, Frank Gerigk et al. 10.1103/Phys. Rev. STAB. 14. 051001
- 9 Liepe M, Stedman G, Valles N. In Proceedings of the 23rd Particle Accelerator Conference. Vancouver, Canada, 2009 (IEEE, Piscataway, NJ, 2009), TU5PFP048
- 10 Jeon D et al. Nucl. Instrum. Methods Phys. Res., Sect. A, 2002, **495**(2): 85. [http://dx.doi.org/10.1016/S0168-9002\(02\)01576-0](http://dx.doi.org/10.1016/S0168-9002(02)01576-0)
- 11 Molloy S. An Empirical Study of HOM Frequencies, ESS-DOCDB (92)
- 12 Schuh M et al. Higher Order Mode Analysis of the SPL Cavities. Proceedings of IPAC'10. Kyoto, Japan, THPE082. 2010. <http://accelconf.web.cern.ch/AccelConf/IPAC10/papers/thpe082.pdf>